Electronic Supporting Information (ESI) for:

Effective Choice of ZnO Formation Methodology for Highly Stable Polymer Solar Cells under Damp-heat (85°C/85%RH) and Light Soaking Conditions

Seung-Hoon Lee, Byoungwook Park, Seung Hun Eom, Seo-Jin Ko, Changjin Lee and Sung Cheol Yoon**

Dr. S.-H. Lee, Dr. B. Park, Dr. S.-J. Ko, Dr. S. H. Eom, Dr. C. Lee, Dr. S. C. Yoon

Division of Advanced Materials, Korea Research Institute of Chemical Technology (KRICT), 141 Gajeong-ro, Yuseong, Daejeon 34114, Republic of Korea
E-mail: cjlee@krict.re.kr, yoonsch@krict.re.kr

Experimental Section

Materials PTB7-Th, EH-IDTBR, PM6, and Y6 were purchased from Derthon Optoelectronic Materials Science Technology (Shenzhen, China). ZnO NPs with sizes of 5–10 nm were synthesized using a previously described method.[1] All other chemicals were purchased from Sigma–Aldrich.

Fabrication of photovoltaic devices Inverted PSCs composed of ITO/ZnO EEL/active layer/MoO_3/Ag were fabricated using the same method as in previous studies.[2, 3] ZnO NPs (25 mg/ml in butanol) were spin-coated onto the ITO patterned substrate at 2000 rpm for 60 s. The Zac-ZnO sol was prepared in air from 0.5M anhydrous Zinc acetate dihydrate and 0.5M ethanolamine in 2-methoxyethanol and spin-coated onto the ITO-patterned substrate at 3000 rpm for 40 s.[4] The pyrophoric diethyl Zn solution (15 wt.% in toluene) was stored in a N_2-filled glove box. The diethyl Zn solution was diluted with tetrahydrofuran (THF) in a glove box for spin coating in air (THF:diethyl Zn = 2:1, total 0.9 ml). The solution (40 μL) was dropped during the rotation of the substrate at 4000 rpm in air. The pipette tips were replaced with new tips each time the solution was coated. The active area of the solar cell is 9 mm^2. The PSCs were encapsulated using a glass cover plate with an ultraviolet curable epoxy and H_2O getter material.

Characterization

J-V, EQE and CELIV measurement The PSCs were characterized by *J–V* curves under dark and AM 1.5 G simulated light irradiation (100 mW cm^{-2}) using a calibrated solar simulator system (Yamashita Denso) and Keithley 2400 instrument. The light intensity was determined using a standard Si solar cell certified by the International System of Units (SI)

(SRC1000 TCKG5N, VLSI Standards, Inc.) and was precisely controlled using a set of two neutral-density filters with six wheels (The 5215 Dual ND Filter Wheel, Newport). For the damp-heat test, a Votch VC7034 climatic chamber was used for the thermal and humidity stress on the PSCs. EQE was measured using a solar cell spectral response/QE/EQE measurement system (QUANTX-300 QE measurement system, Oriel Instruments). The photo-CELIV data were measured using a McScience T4000. The ramp was 5–50 μs and 3 V in amplitude and set to start with an offset matching the V_{oc} of the devices for the delay time.

UV, AFM, UPS and XPS measurement *The 85/85 and photoaged samples preparation* – ZnO and active layer films for analysis after aging were prepared on ITO glass in the same manner when the devices were fabricated. The prepared samples were encapsulated in the same manner as when the PSCs was fabricated using a glass cover plate with UV-curable epoxy and H_2O getter material. The encapsulated samples were aged next to the PSCs in an 85/85 and light-soaking chamber. Before the analysis, we carefully removed the glass cover from the analysis samples.

UV-Vis absorption spectra were measured using a Varian Cary 5000 (Agilent). Height and phase AFM images were obtained using a Nanoscope (Bruker, Inc.). XPS and UPS measurements were carried out using AXIS ultra-delay line detector (DLD) (Kratos, UK) equipped with monochromatic Al Kα (1486.6 eV) as an X-ray source and He I gas (21.22 eV) as a UV source under a vacuum pressure of 5×10^{-8} Torr. The reference Fermi edge for UPS analysis was determined using a cleaned gold surface.

85/85 damp-heat test The 85/85 test was performed using the "ISO-D-3 Damp-heat"[5] method. A Votch VC7034 climatic chamber was subjected to thermal (85°C) and humidity

(85% RH) stress on the PSCs. The devices were measured every 24, 72, and 168 h for 200, 200–500, and 500–1000 h, respectively.

Photoaging test The light-soaking test was performed according to the test ID "ISOS-L-1 Laboratory weathering".[5] A solar-cell reliability system (K3600, McScience) was used. The LG sulfur plasma lamp in the system showed a Class A level spectral match to the AM 1.5G solar spectrum in the visible wavelength range (**Figure S6**). Continuous illumination spontaneously generates thermal radiation in the photovoltaic devices, resulting in a temperature of approximately 40°C. The solar cells were measured automatically every 2, 6, and 12 h for 100, 100–380 and 380–1000 h.

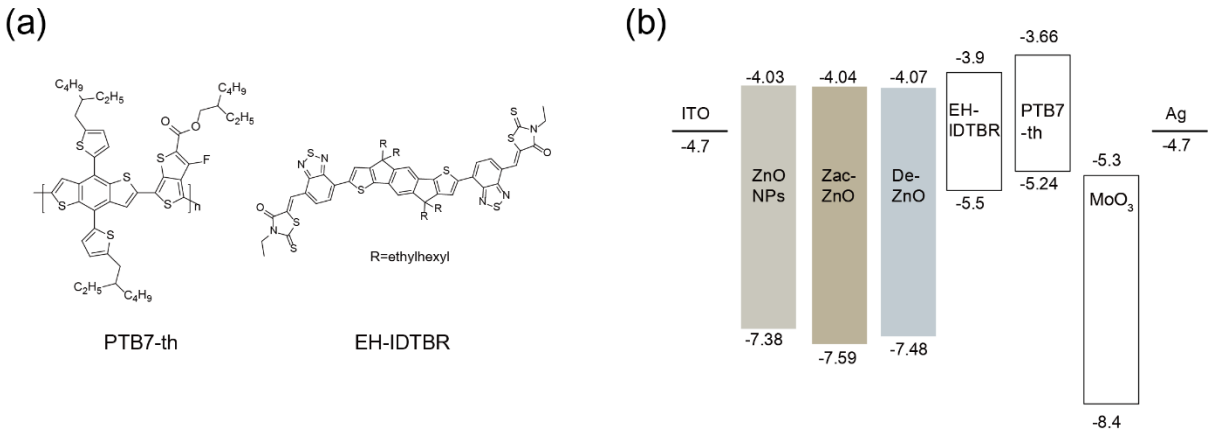

Figure S1. (a) Chemical structures of PTB7-th and EH-IDTBR. (b) Energy diagram of the PSCs using ZnO NP, Zac-ZnO, and De-ZnO. The energy levels and bandgap of ZnOs were measured by UPS, and (UV-Vis) absorption spectroscopy. The energy levels and band gaps of the ZnO EELs were measured by ultraviolet photoelectron spectroscopy (UPS) and ultraviolet and visible (UV-Vis) absorption spectroscopy (Fig. S2 and S3, and Table S2).

Table S1. Photovoltaic parameters of PTB7-th:EH-IDTBR-based PSCs with ZnO NP, Zac-ZnO, and De-ZnO

	V_{oc} [V]	J_{sc} [mA cm^{-2}]	FF [%]	PCE [%]
ZnO NP	1.02	16.20	59.59	9.86
	(1.023 ±0.003)	(15.526 ±0.396)	(59.500 ±0.421)	(9.450 ±0.258)
Zac-ZnO	1.03	16.97	59.43	10.16
	(1.028 ±0.003)	(15.976 ±0.587)	(58.700 ±0.365)	(9.640 ±0.326)
De-ZnO	1.00	16.39	57.25	9.43
	(0.998 ±0.004)	(16.249 ±0.099)	(56.659 ±0.322)	(9.193 ±0.107)

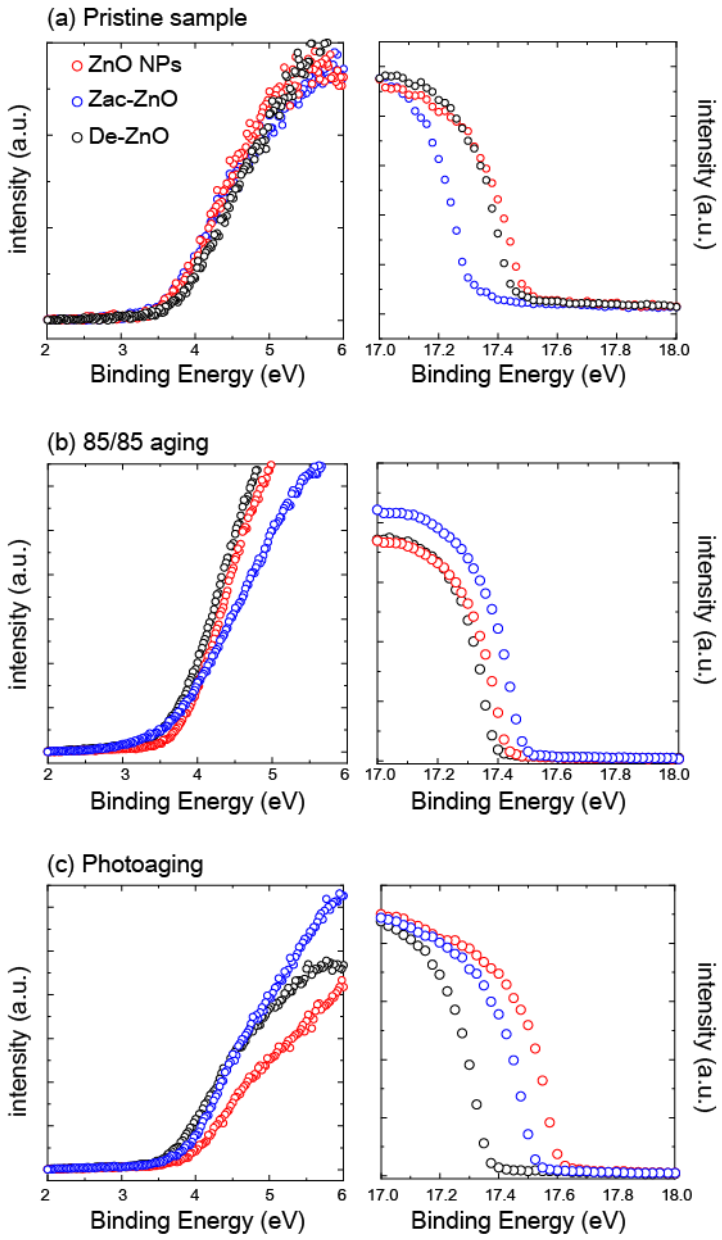

Figure S2. Ultraviolet photoelectron spectroscopy (UPS) spectra of (a) pristine, (b) 85/85 aged and photoaged ZnO EEL films.

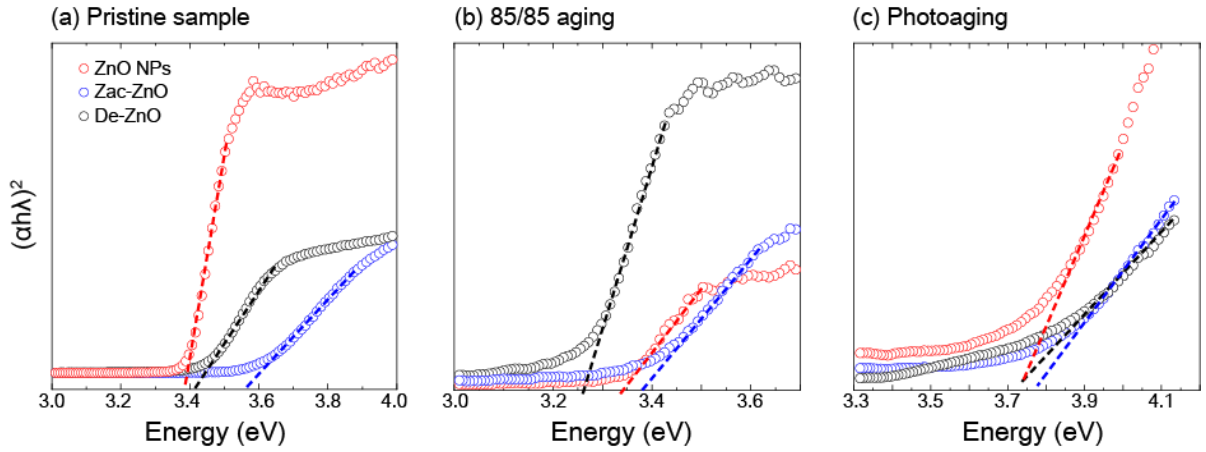

Figure S3. Tauc-plots of (a) pristine, (b) 85/85 aged and (c) photoaged ZnO EEL films

Table S2. VBM, CBM, band gap of of (a) pristine, (b) 85/85 aged and (c) photoaged ZnOs

	VBM (eV)			Band gap			CBM (eV)		
	Pristine	85/85 aging	Photoaging	Pristine	85/85. Aging	Photoaging	Pristine	85/85. Aging	Photoaging
ZnO NPs	-7.38	-7.30	-7.43	3.35	3.34	3.74	-4.03	-4.00	-3.69
De-ZnO	-7.48	-7.32	-7.44	3.41	3.25	3.74	-4.07	-4.07	-3.7
Zac-ZnO	-7.59	-7.51	-7.47	3.55	3.36	3.78	-4.04	-4.15	-3.69

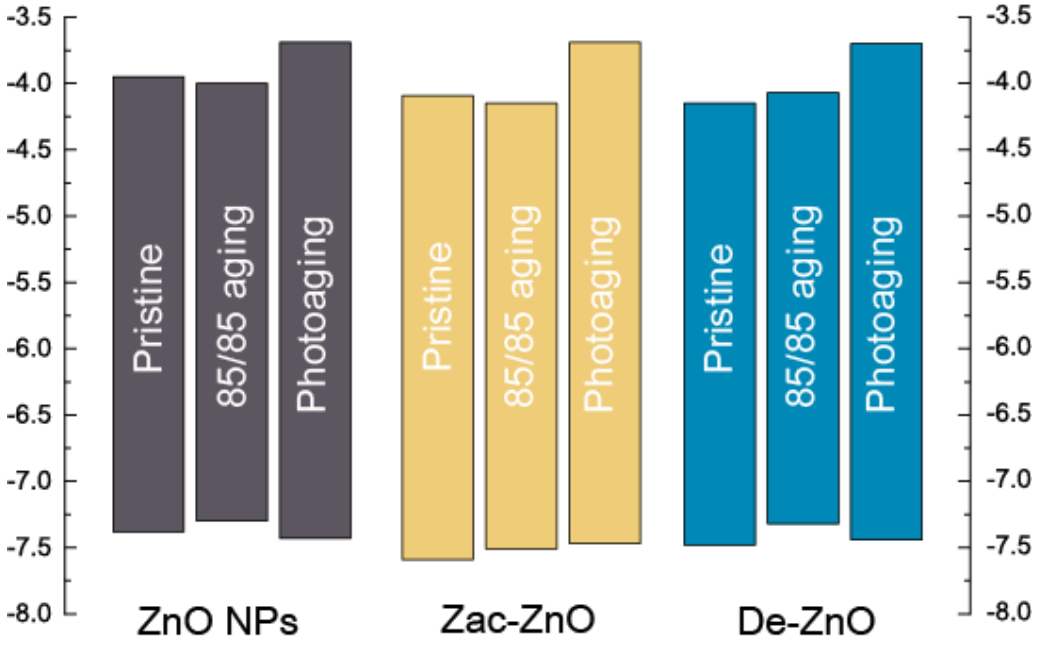

Figure S4. Energy levels of pristine, 85/85 aged and photoaged ZnOs

UPS and UV-vis absorption spectroscopy were performed to evaluate energy levels and band gap of the ZnO EELs before and after 85/85 aging and photoaging (Fig. S1-S3 and Table S1). Typically, the valence band maximum (VBM), the conduction band minimum (CBM), and band gap (E_g) of ZnO are -7.8 eV, -4.4 eV, and 3.4 eV.[6] The VBM, CBM of the ZnO NP, Zac-ZnO and De-ZnO were evaluated slightly shallower than literature values. It is attributed to low temperature annealing (130ºC) and fabricated from solution.[7-9] The E_g of all the ZnO films are similar to literature values. After 85/85 aging and photoaging, the summary of energy levels is shown in Fig. S3 and Table S1. The light and damp-heat source lead to change the energy levels and E_g. It might be attributed to variation of the stoichiometry of ZnO films. Especially, the photo-aging induces a wider E_g than fresh ZnO, which indicates that the increase of the point defects.[10, 11] The increase of defects might be associated with the increase of oxygen defect in XPS spectra. Similar to devices results, photo source damages the ZnO films more than 85/85 condition.

Figure S5. The images of photostability measurement system.

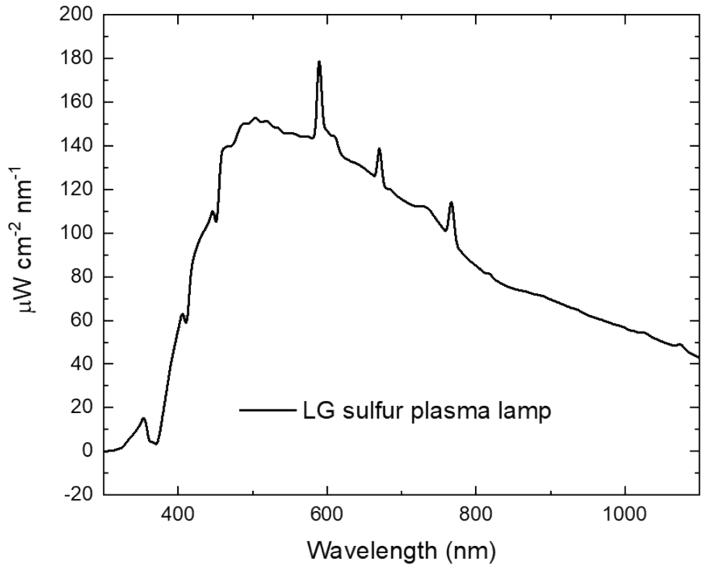

Figure S6. Light spectrum of the sulfur plasma lamp used in this work as extracted from the company's datasheet

Table S3. The specifications and spectral match of sulfur plasma lamps from the company's datasheet

Wavelength	Spectral Match	Class
400-500	0.9	A
500-600	1.09	A
600-700	1.03	A
700-800	1.02	A
800-900	0.88	A
900-1100	1.04	A
Class	A	

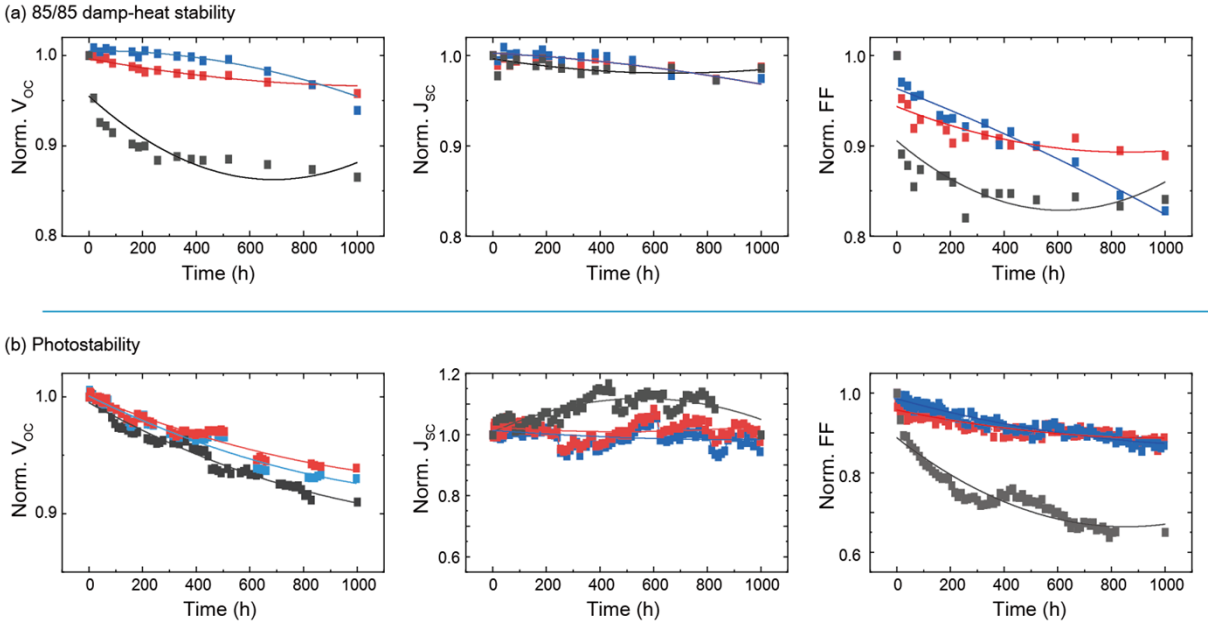

Figure S7. V_{oc}, J_{sc}, and *FF* degradation curves of over 1000 h under continuous (a) 85/85, and (b) light-soaking condition. The curves are each normalized the initial value of pristine devices.

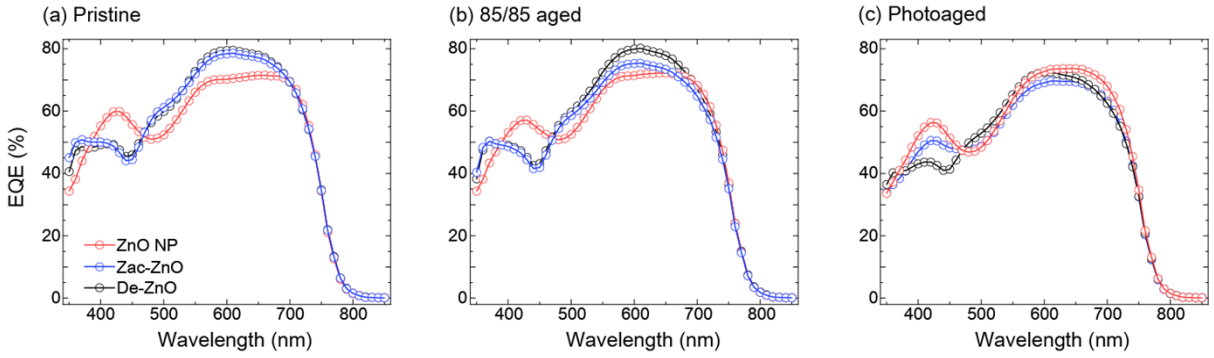

Figure S8. The EQE spectra pristine, 85/85 aged and photoaged devices with ZnO NP, Zac-ZnO and De-ZnO.

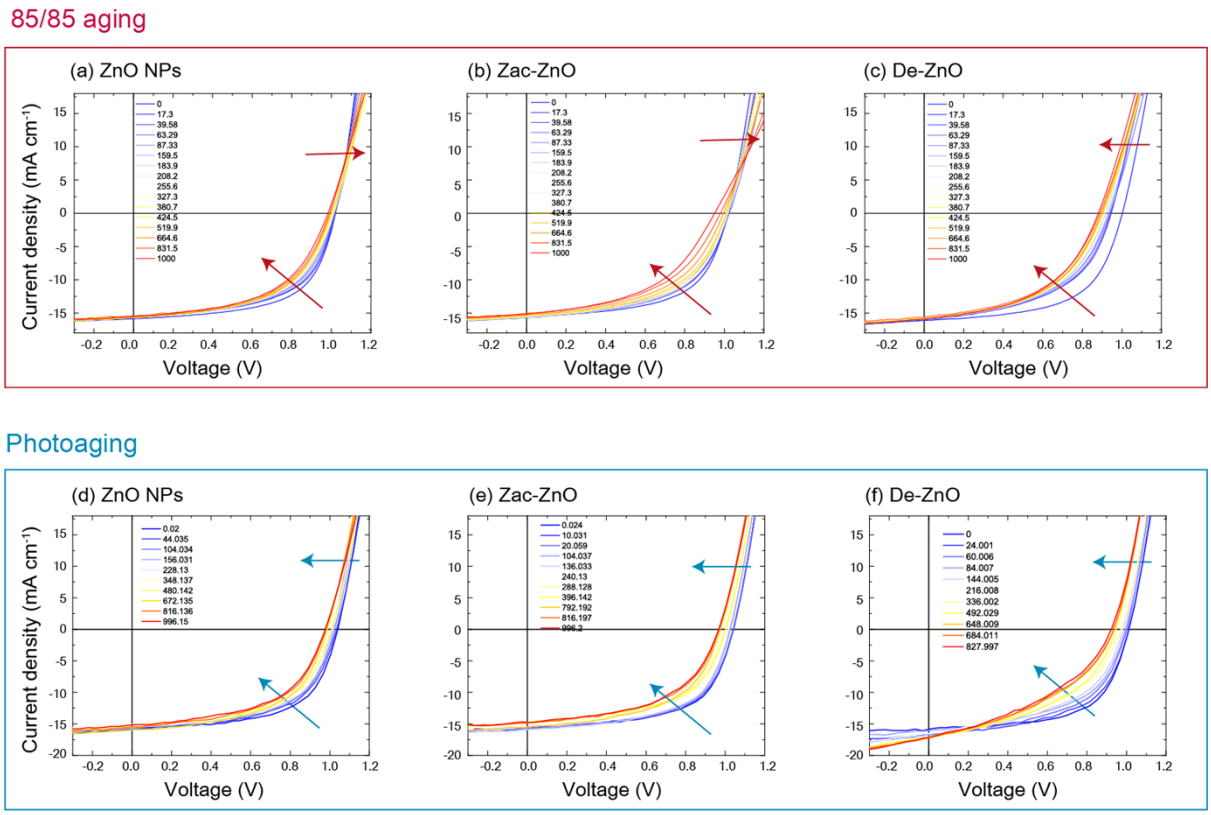

Figure S9 . The *J-V* curves of the PSCs with (a,d) ZnO NPs, (b,e) Zac-ZnO and (c,f) during 85/85 aging and photoaging.

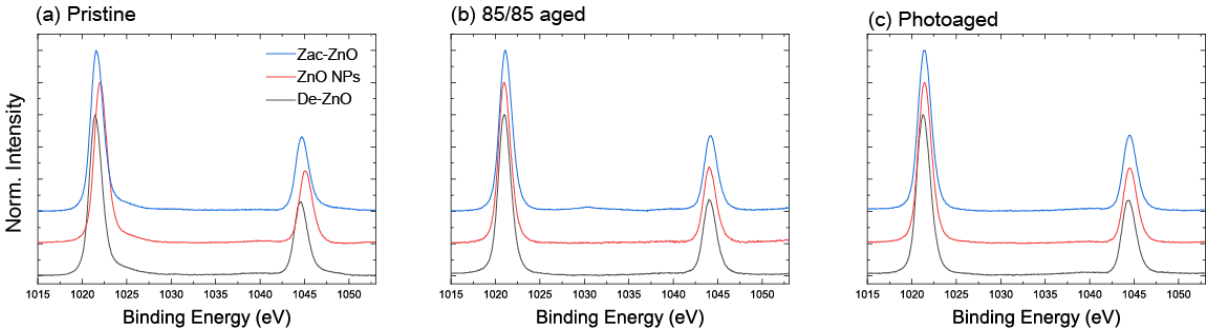

Figure S10. XPS spectra of Zn 2p of (a) pristine, (b) 85/85 aged and photoaged ZnOs. The Zn 2p core-level of ZnO films has two peaks located at approximately 1044 and 1021 eV attributed to Zn $2p_{1/2}$ and Zn $2p_{3/2}$, respectively.

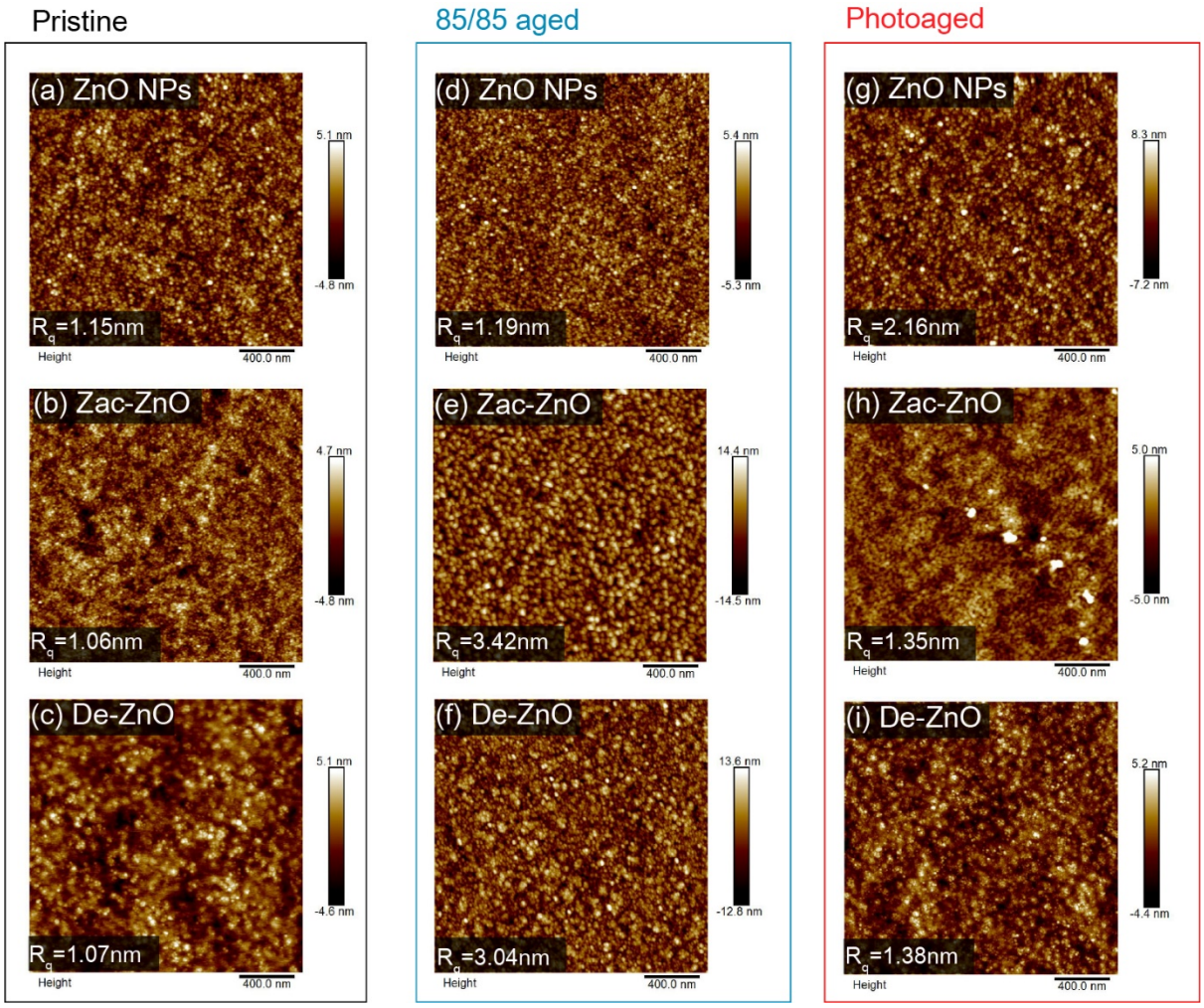

Figure S11. AFM images of pristine, 85/85 aged, and photoaged (a,d and g) ZnO NPs, (b,e and h) Zac-ZnO and (c,f and i) De-ZnO

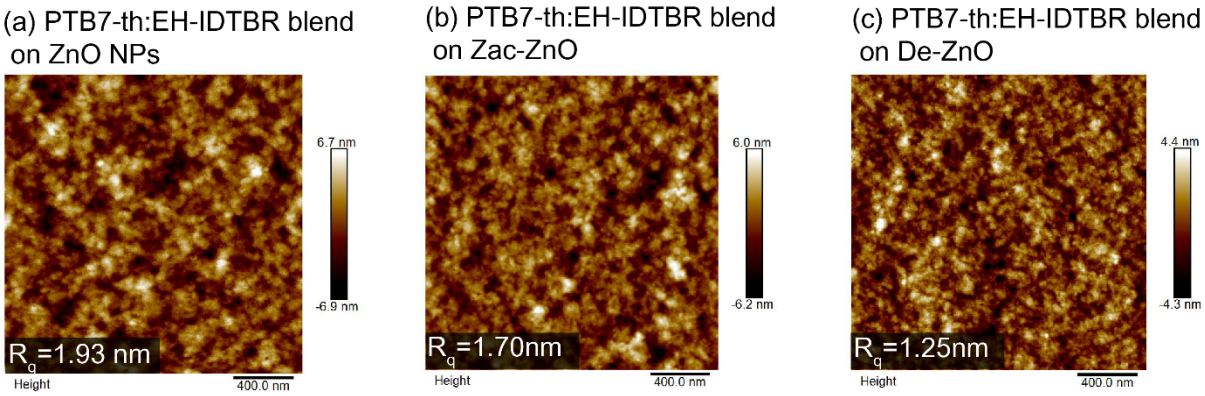

Figure S12. The surface morphologies of PTB7-th:EH-IDTBR blend films on (a) ZnO NPs, (b) Zac-ZnO and (c) De-ZnO measured by AFM

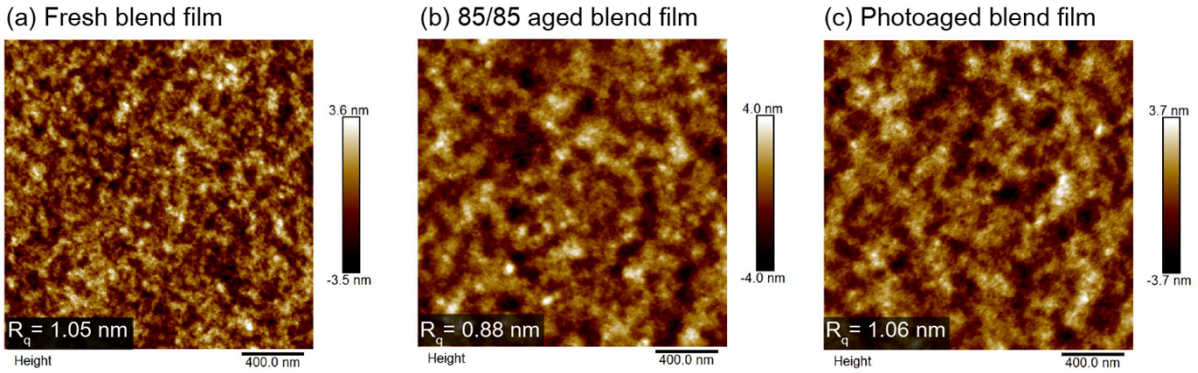

Figure S13. The AFM images of PTB7-th:EH-IDTBR blend films (a) pristine and (b) after 85/85 and (c) photoaging

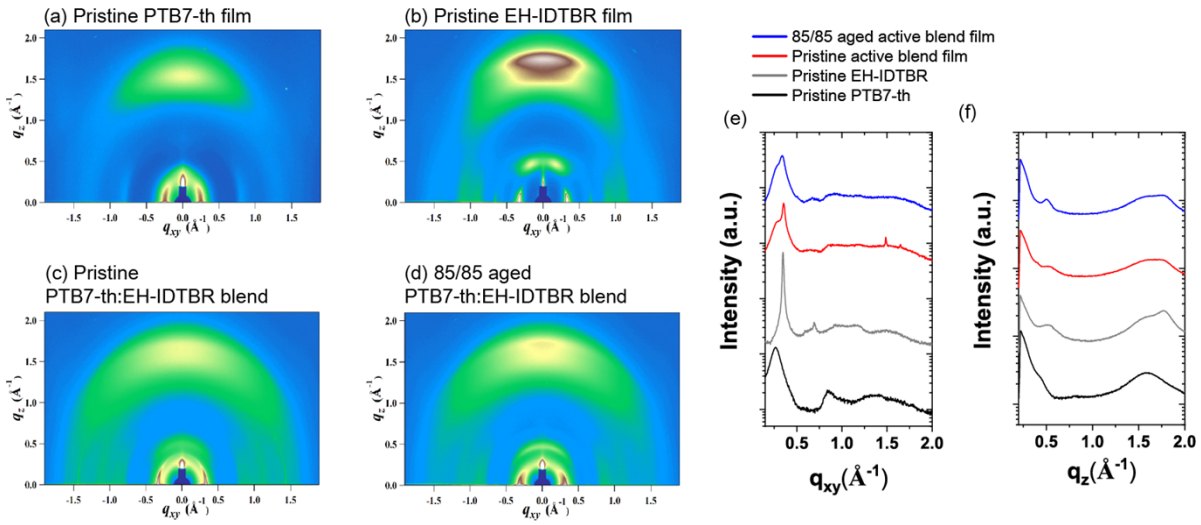

Figure S14. 2D GIWAXS scattering patterns of (a) pristine donor, (b) acceptor, (c) fresh blend film, and (d) 85/85 aged blend film. (e) In-plane and (f) out-of-plane linecuts of 2D GIWAXS of the active films

The active blend films exhibit in-plane (IP) q value at ~0.36 $Å^{-1}$ for lamellar stacking originated from the lamellar stacking of the EH-IDTBR. In out-of-plane (OPP), q value at ~ 1.7 $Å^{-1}$ for the (010) diffraction peaks of blend film also mainly derive from the EH-IDTBR.

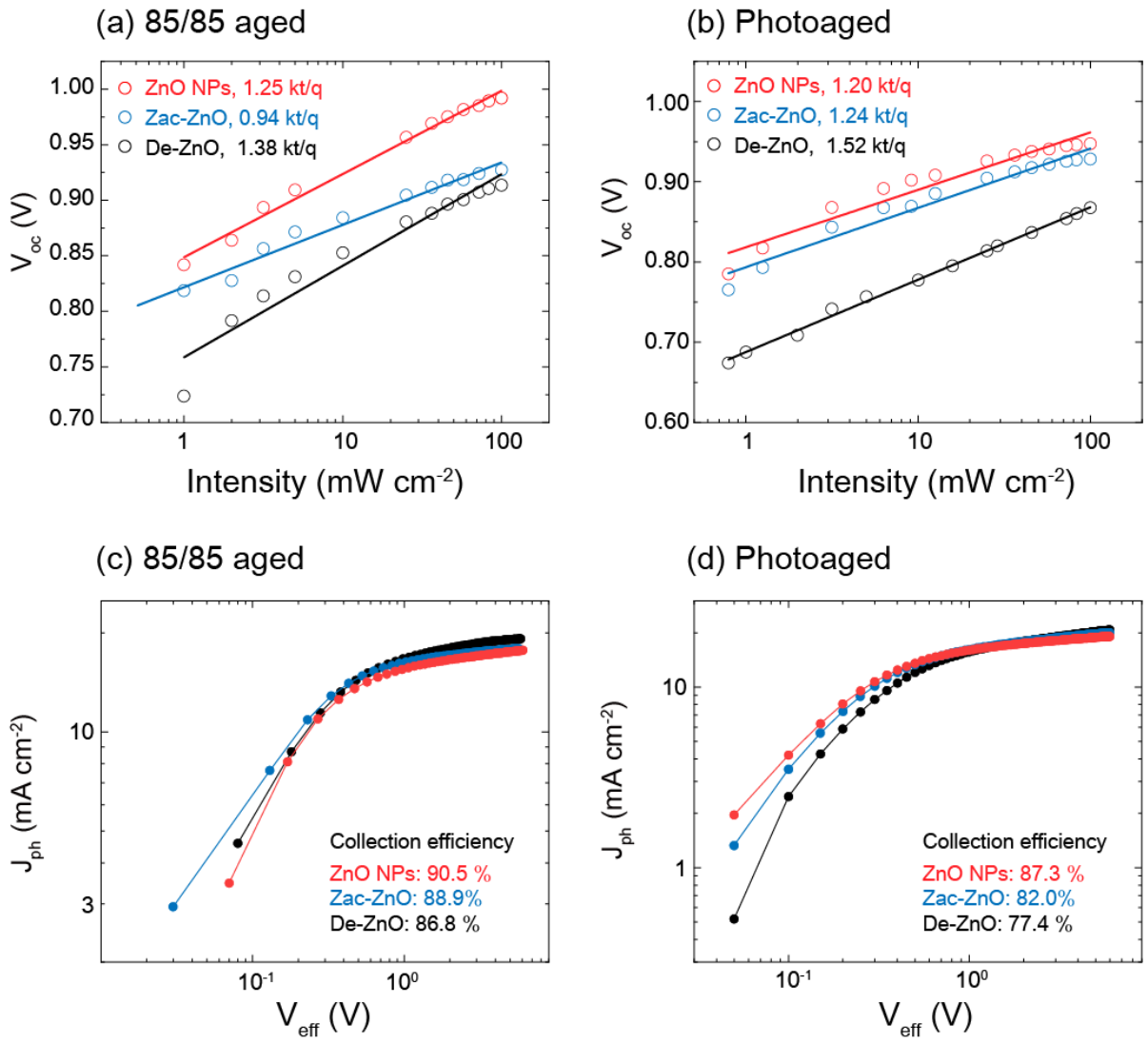

Figure S15. Open-circuit voltage as a function of light intensity, photocurrent density vs. effective voltage (J_{ph}-V_{eff}) characteristics for the (a and c) 85/85 and (b and d) photoaged PSCs with ZnO NP, Zac-ZnO, and De-ZnO.

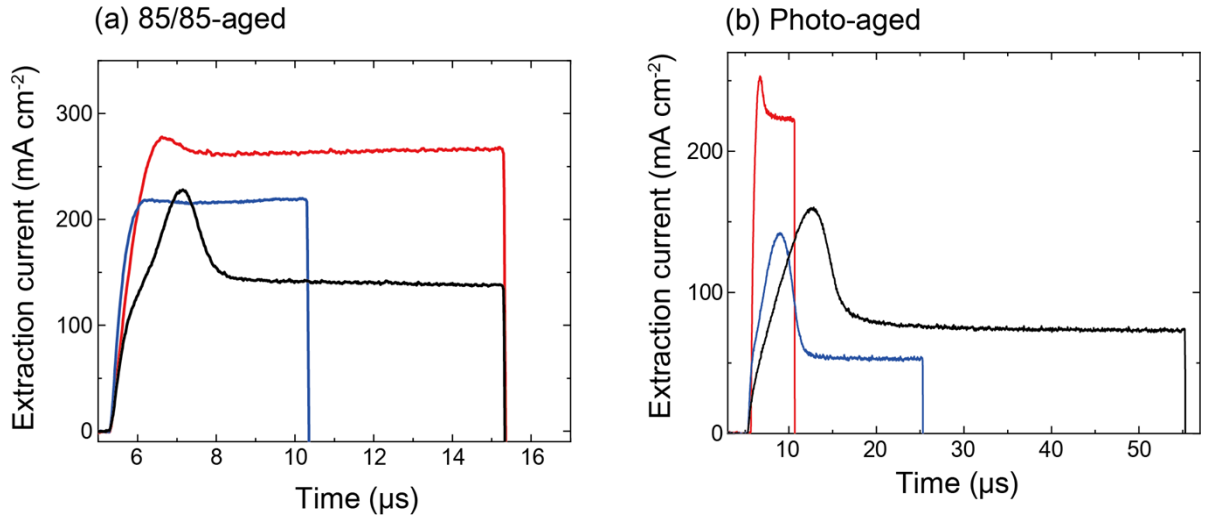

Figure S16. Photo-CELIV transients for the (a) 85/85 and (b) photoaged PSCs with ZnO NP, Zac-ZnO, and De-ZnO.

The maximum current peak and the area formed by photoexcitation of the 85/85 aged and photoaged PSCs increased, indicating an increase in the extracted charge carrier. The increase in the charge carrier originates from the traps generated by the aging process, which agrees with the results of the dominant trap-assisted recombination.[11]

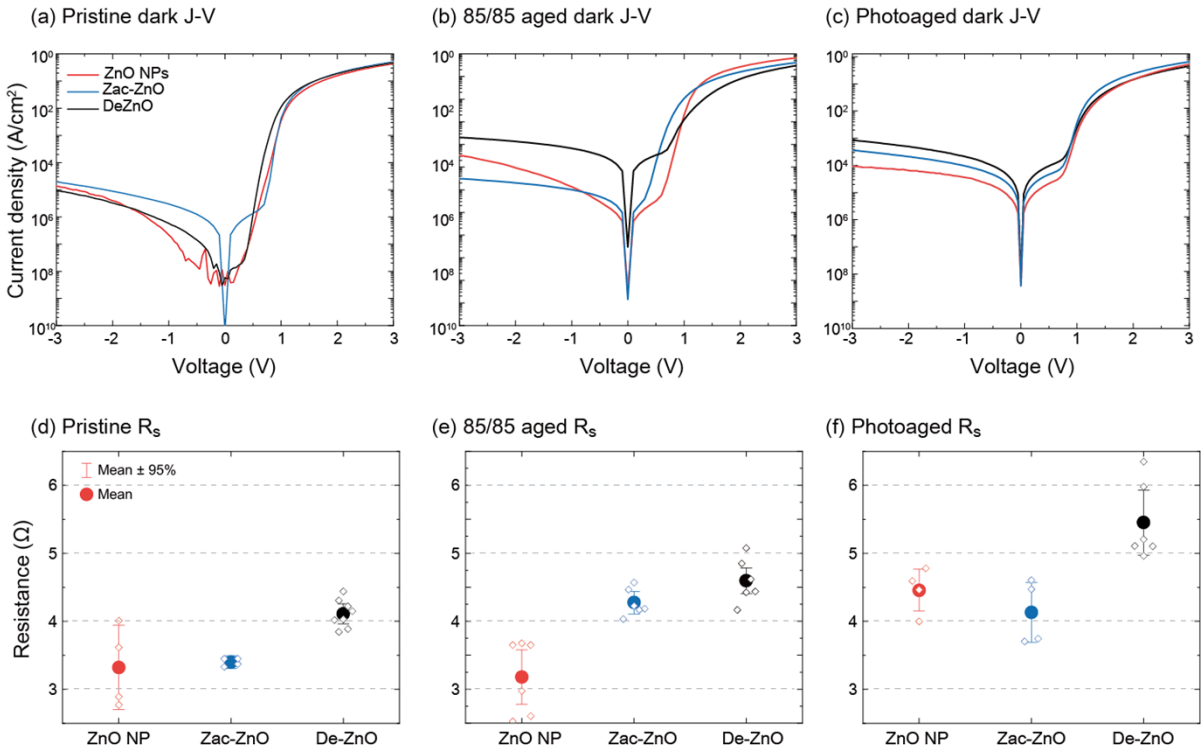

Figure S17. Series resistance (a), (b), and (c) of pristine, 85/85, and photoaged devices extracted from dark *J-V* curves of Fig. 5(a) – (c).

The R_s (3.40 Ω cm^{-2}) of the fresh PSCs with ZnO NPs is similar to that of the 85/85 aged sample (3.61 Ω cm^{-2}) and slightly lower than that of the photoaged devices (4.45 Ω cm^{-2}). The R_s of devices with Zac-ZnO after 85/85 (4.16 Ω cm^{-2}) and photoaging (4.13 Ω cm^{-2}) were slightly higher than those of fresh samples (3.40 Ω cm^{-2}). The R_s (4.04 Ω cm^{-2}) of fresh solar cells with De-ZnO is higher than those of fresh solar cells with other ZnOs. Further, the R_s of the device with De-ZnO after 85/85 and photoaging were 4.30 and 5.45 Ω cm^2, respectively.

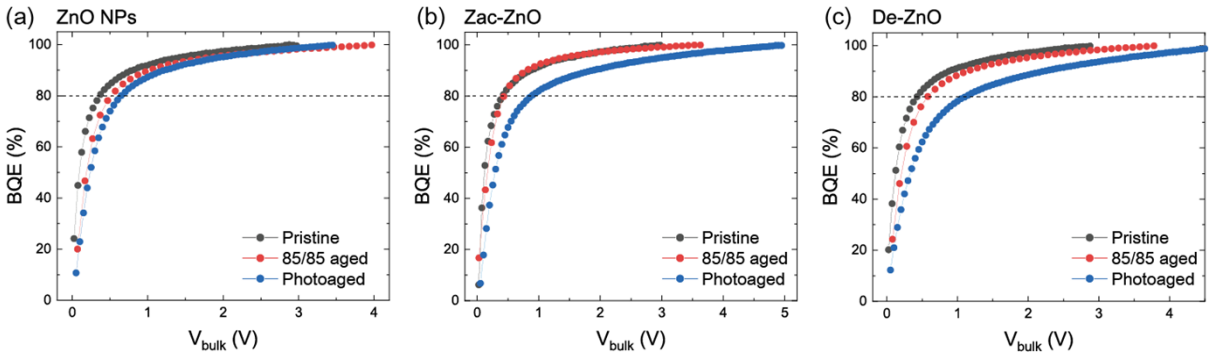

Figure S18. BQE-V_{bulk} characteristics of pristine, 85/85 aged and photoaged PTB7-th:EH-IDTBR devices with (a) ZnO NP, (b) Zac-ZnO and (c) De-ZnO.

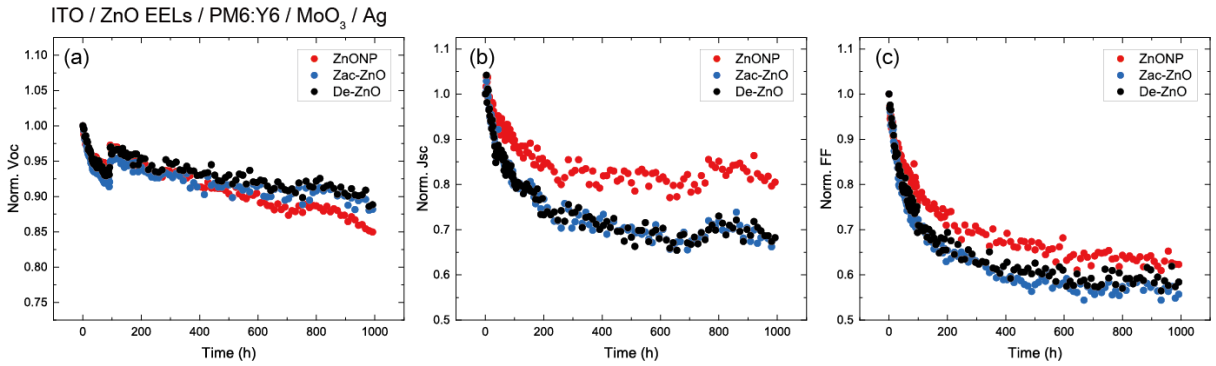

Figure S19. The normalized V_{oc}, J_{sc} and *FF* measured for the PM6:Y6 PSCs as a function of aging time under 1 sun illumination with class A level.

References

1. W. J. Beek, M. M. Wienk, M. Kemerink, X. Yang and R. A. Janssen, *J. Phys. Chem. B*, 2005, **109**, 9505-9516.

2. S.-H. Lee, S.-J. Ko, S. H. Eom, H. Kim, D. W. Kim, C. Lee and S. C. Yoon, *ACS. Appl. Mater. Interfaces*, 2020, **12**, 14244-14253.

3. J.-J. Park, Y.-J. Heo, J.-M. Yun, Y. Kim, S. C. Yoon, S.-H. Lee and D.-Y. Kim, *ACS. Appl. Mater. Interfaces*, 2020, **12**, 42811-42820.

4. Y. Sun, J. H. Seo, C. J. Takacs, J. Seifter and A. J. Heeger, *Adv. Mater*, 2011, **23**, 1679-1683.

5. M. O. Reese, S. A. Gevorgyan, M. Jørgensen, E. Bundgaard, S. R. Kurtz, D. S. Ginley, D. C. Olson, M. T. Lloyd, P. Morvillo, E. A. Katz, A. Elschner, O. Haillant, T. R. Currier, V. Shrotriya, M. Hermenau, M. Riede, K. R. Kirov, G. Trimmel, T. Rath, O. Inganäs, F. Zhang, M. Andersson, K. Tvingstedt, M. Lira-Cantu, D. Laird, C. McGuiness, S. Gowrisanker, M. Pannone, M. Xiao, J. Hauch, R. Steim, D. M. DeLongchamp, R. Rösch, H. Hoppe, N. Espinosa, A. Urbina, G. Yaman-Uzunoglu, J.-B. Bonekamp, A. J. J. M. van Breemen, C. Girotto, E. Voroshazi and F. C. Krebs, *Sol. Energy. Mater. Sol. Cells*, 2011, **95**, 1253-1267.

6. Z. Liang, Q. Zhang, L. Jiang, G. Cao, *Energy. Environ. Sci*, 2015, **8**, 3442-3476.

7. A. Sharma, S.E. Watkins, G. Andersson, D.A. Lewis, *Energy. Technol.*, 2014, **2**, 462-468.

8. S. Gutmann, M. Conrad, M. Wolak, M. Beerbom, R. Schlaf, *J. Appl. Phys*., 2012, **111** 123710.

9. Y.-S. Jung, J.-S. Yeo, B.-K. Yu, D.-Y. Kim, *Sol. Energy. Mater. Sol. Cells*, 2015, **134,** 291-297.

10. R. Al-Gaashani, S. Radiman, N. Tabet, A. Daud, *Mater. Sci. Eng. B Solid State Mater Adv Technol*, 2012, **177**, 462-470.

11. X. Du, T. Heumueller, W. Gruber, A. Classen, T. Unruh, N. Li, C.J. Brabec, *Joule.*, 2019, **3**, 215-226.